# Enhancement effect of Au claddings in tip enhanced Raman spectroscopy

Zhang, Yuquan; Cao, Liwei; Chen, Houkai; Dai, Yanmeng; Man, Zhongsheng; Li, Guang; Min, Changjun; Urbach, H. P.; Yuan, Xiaocong

**DOI**
10.1016/j.ijleo.2019.163326

**Publication date**
2019

**Document Version**
Final published version

**Published in**
Optik

**Citation (APA)**
Zhang, Y., Cao, L., Chen, H., Dai, Y., Man, Z., Li, G., Min, C., Urbach, H. P., & Yuan, X. (2019). Enhancement effect of Au claddings in tip enhanced Raman spectroscopy. *Optik*, *199*, Article 163326. https://doi.org/10.1016/j.ijleo.2019.163326

Optik - International Journal for Light and Electron Optics 199 (2019) 163326

Contents lists available at ScienceDirect

Optik

journal homepage: www.elsevier.com/locate/ijleo

Original research article

# Enhancement effect of Au claddings in tip enhanced Raman spectroscopy

Yuquan Zhang[a], Liwei Cao[a], Houkai Chen[a], Yanmeng Dai[a], Zhongsheng Man[b,c], Guang Li[a], Changjun Min[a,*], H.P. Urbach[b], Xiaocong Yuan[a,*]

[a] Nanophotonics Research Center, Shenzhen Key Laboratory of Micro-Scale Optical Information Technology, Shenzhen University, Shenzhen 518060, China
[b] Optics Research Group, Delft University of Technology, Lorentzweg 1, 2628CJ Delft, the Netherlands
[c] School of Physics and Optoelectronic Engineering, Shandong University of Technology, Zibo 255000, China

ARTICLE INFO

*Keywords:*
Tip enhanced Raman spectroscopy
Atomic force microscopy
Enhancement factor
Metal cladding

ABSTRACT

The tip-enhanced Raman spectroscopy (TERS) provides a non-destructive and label-free molecular detection approach with high sensitivity due to the hotspot excited at tip apex, which depends crucially on the tip parameters. Here, we employed an Au cladded atomic force microscopy probe to investigate enhancement effect of the Au claddings, both in theories and experiments. The simulation optimized a highest enhancement with Au cladding thickness of 50 nm under given experimental condition, being consistent with the experimental results. It provides a practical guide to optimize the probes to improve the TERS sensitivity and exert potentials in further TERS applications.

## 1. Introduction

Tip enhanced Raman spectroscopy (TERS) offers a valuable approach to characterize the molecular chemical and physical properties, where the tip functions as the enhancing unit to provide an ultra-high sensitivity within a nano-size [1–5]. As an active non-destructive and label-free molecular detecting approach, TERS has been widely employed in many researches [6–11], such as biochemical analysis, materials characterization, and others. In TERS systems, due to the hybrid coupling effect between the metal probe and excitation beam, localized surface plasmon resonance (LSPR) could be excited at the tip [12–16], which directly contributes to the enhancement of electromagnetic field and Raman signals. The high sensitivity is highly depended on parameters of the probe [17], e.g. size and shape. Consequently, an effective nano-probe is of crucial importance for TERS researches.

The silicon atomic force microscopy (AFM) probes with metallic cladding are usually employed in TERS researches [18–20]. The probes usually need modification as the enhancement is closely related with the tip, and many approaches have been proposed and demonstrated for a higher sensitivity [21–27], such as electrochemical etching, chemical vapor deposition, thermal evaporation, fabrication of nanostructures on the tip, and so on. Then Raman signals can strongly be enhanced through excited localized hotspot on the metallic cladding. As the simplest approach, the vacuum deposition technique provides a convenient physical process to get a relative smooth metallic surface by lowing the deposition rate with high repeatability [28]. As has been demonstrated previously, the physical parameters, including the tip radius, tip angle, morphology, etc., exert great influences on the localized field distribution and final Raman spectral intensities [29–31]. Consequently, it is necessary to quantify the enhancement under different cladding

* Corresponding authors.
*E-mail addresses:* cjmin@szu.edu.cn (C. Min), xcyuan@szu.edu.cn (X. Yuan).

https://doi.org/10.1016/j.ijleo.2019.163326
Received 16 May 2019; Received in revised form 26 August 2019; Accepted 29 August 2019

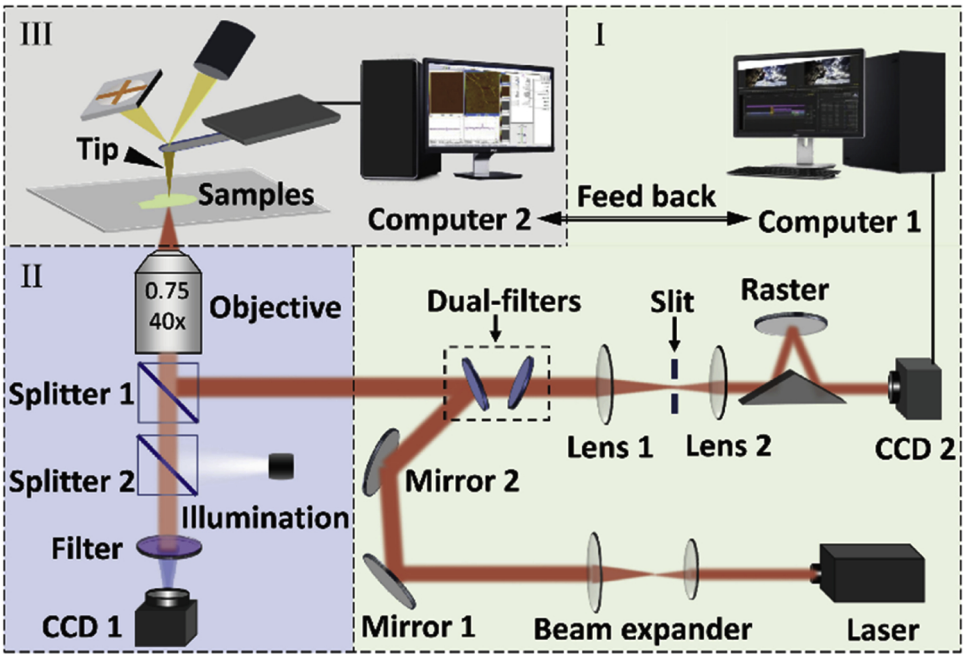


**Fig. 1.** Schematic of the AFM- based TERS configuration, which is combined by Renishaw inVia Raman system (Part I), Nikon microscope system (Part II), and the Bruker Catalyst system (Part III).

parameters to provide guidance for optimization of further TERS detections.

Here, we investigate the influence of Au cladding on enhancement of a TERS system. An inverted AFM-based TERS setup with illumination from the bottom was employed. A gold layer with different thicknesses is cladded on the tip of the AFM probe by thermal evaporation method, then hotspot could be excited when the probe is located in the focused laser field. To get a sufficiently effective detection, we located the tip at the position of longitudinal component, which could excite hotspot on the apex point completely in the gap between the tip and substrate. Numerical simulations about the field distribution and intensity are performed by the finite difference time domain (FDTD) method, and Raman signals are experimentally detected for analysis. The simulations demonstrated that the cladding thickness has high effect on the Raman spectrum enhancement, and the intensity peaked at thickness of 50 nm under experimental conditions, in accordance with the detected results. It gives out a practical guide to optimize the probes to improve the TERS sensitivity and could exert great potentials in further TERS applications.

## 2. Experimental setup and methods

An integrated AFM-Raman detection system was established firstly for optimization, by coupling a Bruker Catalyst system onto a Nikon microscopy frame, together with a Renishaw inVia Raman system, as shown in Fig. 1. The AFM probe is attached on a two-dimensional motorized precision translation stage to accommodate its position to couple with the exciting laser: a linearly polarized 632.8 nm beam focused by a 40× objective with NA of 0.75 from the bottom. The incident laser beam is expanded firstly through a telescopic system to fit back aperture of the objective lens, and then be focused onto tip of the AFM probe. Samples are placed on a glass substrate and actuated by a piezoelectric mapping stage inserted in a motorized stage. Subsequently, an enhanced Raman spectrum could be excited when the tip is near to the samples. The back-scattered TERS signals can be collected by the objective and diffracted through the raster to be measured by the Renishaw system (CCD2), as shown in part I of Fig. 1. In experiments, actuator of the AFM maintains alignment with the spectrometer and stage, to get a synchronous measurement. In addition, a white-light source illuminates the sample and probe from the bottom to capture the experimental process by a CCD camera (CCD1), as well as the back-scattered light by apex of the tip through the same objective, which assists to locate the probe.

The coating material is important for AFM tips, which contributes to the excitation of plasmonic hotspots. Here, we chose Au as the cladding material as it is not so active to be oxidized compared with Ag. The schematic of the Au cladded AFM probe for TERS detection is shown in Fig. 2a and b. The probe (Nanosensors Inc.) is silicon-based with a cone angle of 30° ($\varphi$) and tip radius of 10 nm ($r_2$), and the angle between probe and substrate is approximately 50° ($\theta$). To provide higher enhancement, the silicon probes were further modified by an Au cladding (Au purity of 99.999%). The claddings then change the radius of the tip ($r_1$), to exert great influences on excited Raman signals. Experimentally, the tips were coated using an evaporation system at $5 \times 10^{-5}$ Torr nitrogen, where the tips were located on an inverted substrate. The deposition velocity was set as 0.02 nm/s by regulating the current to get a relative smooth Au coating. Fig. 2c shows the SEM image of the modified probe, where a uniform Au cladding could be obviously observed, as the arrows indicated. The coated tips were stored in a vacuum tank and used within several days.

For calibration of the TERS system, a sample of uniform 4-nitrobenzenethiol molecule layer was employed to study enhancement

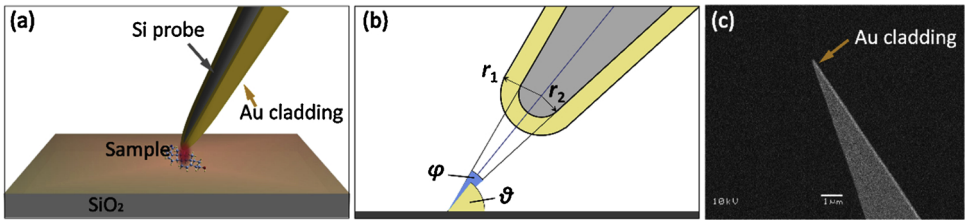


**Fig. 2.** (a) 3D schematic of the TERS detection system, cutaway view of the probe shows Au cladded silicon AFM tip. (b) 2D model for simulations, $\varphi$ is the cone angle of the probe and $\theta$ is the tilt angle with the substrate platform. (c) Side-view SEM images of a tip vapor-coated with a thin layer of gold under magnification of 1000×.

effect of Au cladding thickness on Raman signal. The powdery sample was firstly dissolved in alcohol, and diluted to a low concentration of $10^{-6}$ M. The sample solution was symmetrically spin-coated onto a glass substrate in a spinner with rotational speed of 5000 rpm, and then reposed till complete evaporation. For measurements, samples were located on the stage, the Raman signals could be detected when the probe was contacted with the sample. Based on these, enhancement effects could be compared to get an optimized parameter of tips.

## 3. Results and discussions

The TERS effect essentially stems from the hotspots with excited LSPR at the apex of metal probe. To evaluate the physical process, we numerically analyze the electric field distribution around the Au cladded tip by a 3D finite-difference time-domain (FDTD) method model. Here, we process the focusing of incident light using the Richards–Wolf vectorial diffraction theory [32] to calculate the focused electric field near the focal region. When the Au-coated probe is illuminated by a focused laser, the localized surface plasmons are excited on the tip, resulting in the creation of hotspots to generate enhanced Raman scattering from a sample. The hotspot on the tip depends largely on field distribution of the focus, which is in high reliant on the polarization [33]. For a linearly polarized laser, its intensity distribution at the focus spot has an elliptical shape, with a transverse component at the center and two longitudinal components symmetrically along the polarized direction. It has been demonstrated that the hotspots could be excited on the sides of the tip instead of the apex point when the tip is located at the center [33] where the transverse component dominated. It is clear that it was not a sufficiently effective way for detection of molecules located in the gap between the tip and substrate. Consequently, in this work, we located the tip at the longitudinal maxima point, to excite hotspot at the very apex point of the probe.

The field enhancements of probes with different Au coating thicknesses were analyzed compared with the results without cladding firstly. In accordance with experimental conditions, we consider the tip as a silicon circular cone (cone angle $\varphi = 10^{\circ}$, tilted angle $\theta = 50^{\circ}$) cladded with different Au coating thicknesses ($r_1$-$r_2$). The Au cladding leads to an increased apex radius, which is equivalent to the thickness. All other parameters keep in accordance with experiments. The outer Au coating with thickness from 0 to 110 nm are simulated to optimize the enhanced intensity of excited hotspot, as shown in Fig. 3. The results proved that thickness of Au cladding produces strong influences on the field enhancement, which is peaked at 50 nm under the experimental conditions.

Furthermore, the simulations demonstrated an enhanced field being excited at the interface between the Si probe and Au

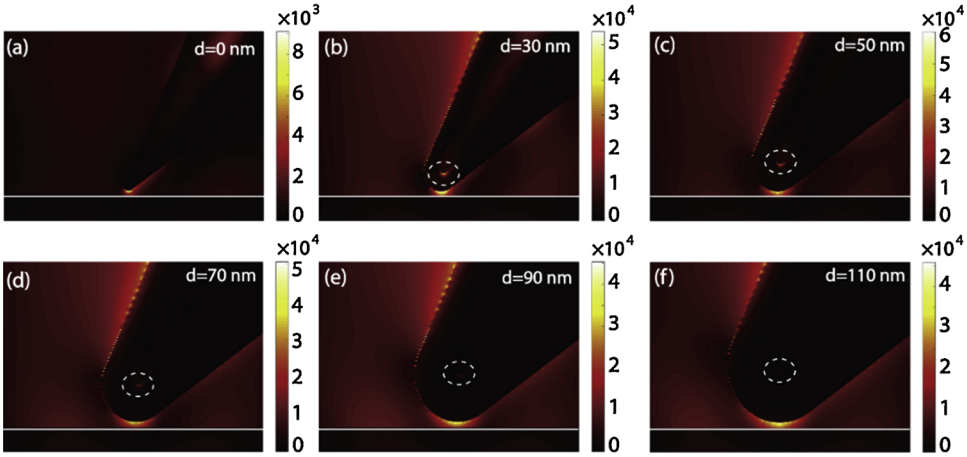


**Fig. 3.** Simulative results of tip enhanced electric field intensity distributions with different cladding thickness of 0, 30, 50, 70, 90, and 110 nm, respectively. Enhanced field is achieved in the gap between the tip and glass substrate. White lines indicate the interface of substrate, dashed circles show the enhanced localize electronic field at the interface between Si probe and Au cladding.

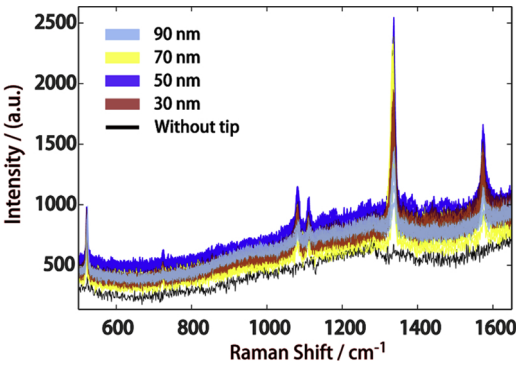


**Fig. 4.** Measured Raman spectrum of 4-nitrobenzenethiol with different Au cladding thicknesses (colored areas), and the signals with the tip withdrawn (black line) for comparison. The colored areas are composed with ~20 independent curves.

cladding, as indicated in the dashed circles in Fig. 3. As thin Au coating could be polarized to generate opposite charges at the Air-Au and Au-Si interfaces, therefore, parts of the energy are divided by the Au-Si interface. Naturally, its intensity decreases with a thickened cladding. However, the hotspot at the Au-Si interface is failed to contribute to the Raman signal detection as it is isolated by the Au cladding. As a result, a parabolic enhancement at the tip with gradually increased cladding thickness could be achieved, to highly enhance Raman signals of the samples located in the gap for detection.

To verify the above simulation results, Raman signals are detected experimentally, with a linearly polarized 632.8 nm laser (60 μW) being focused through an objective with NA of 0.75. The tip is aligned on a two-dimension mechanically movable platform, to align with the laser focus. When the probe scans through the focused field, a scattered signal could be captured by the CCD and detected by the spectrometer, with a brightest signal at the center. Then, the probe was moved along the polarization with 300 nm to align with the longitudinal component position to excite hotspot exactly in the gap between the tip and substrate. Fig. 4 shows the Raman spectrum signal intensity with Au thickness of 30, 50, 70, and 90 nm, respectively, as well as the spectrum with probe withdrawn (the black line) as a comparison. The results demonstrated a better enhancement at the optimized cladding thickness of 50 nm. The measured results with cladded probes were repeated at ~20 random positions to reduce the errors, with exposure time of 1 s for each point. It is easy to find that the sample's Raman spectrum is difficult to measured when the probe is withdrawn, but it could be highly enhanced by excited hotspot and thus easily detected when the tip is closed to the sample surface. From the simulative and experimental results above, a relative better parameter under the given condition could be achieved with a higher enhancement.

In addition to the curvature induced by claddings, many other characteristic parameters of the probe, such as the tilt ($\theta$) and cone angles ($\varphi$), also exert big influence on the field enhancement. On account of this, we show the influences of such two parameters in Fig. 5, with Au thickness of 50 nm. The results demonstrate that the hotspot could also be created at the tip of probe, just in the gap between probe and the glass substrate. The enhanced field intensity decreases with both increased tilt angles (Fig. 5a–d) and cone angles (Fig. 5e–h). That is, for a probe with fixed radius of curvature, a vertical tip with smaller cone angle will bring higher enhancement.

Except for the above parameters, roughness of the probe could also exert direct influences on the Raman enhancement. As it could be reduced experimentally through lowing the deposition velocity and add an annealing process after coating of the claddings, it is not taken into consideration here for simplification. Furthermore, distribution and intensity of the focus field also exerts important influence for the enhancement [34,35], as it is depended by polarization and phase of the incident light. As a result, there also exist

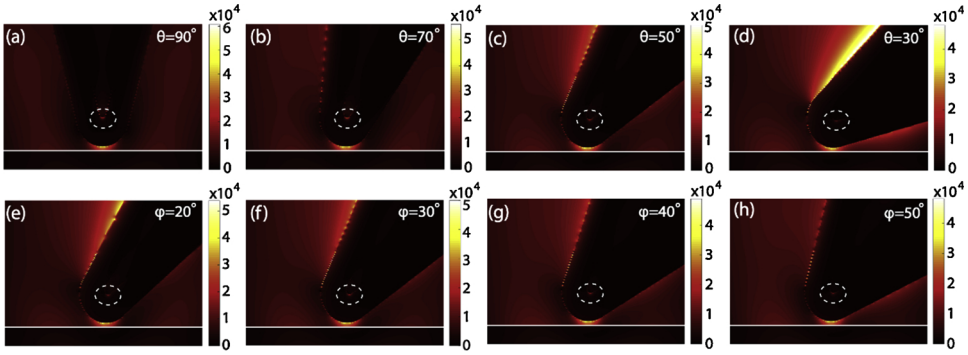


**Fig. 5.** Simulated tip enhanced electric field distributions of cladded probes with tilt angles (a–d) and cone angles (e–h). a–d are the results with tilt angles of 90°, 70°, 50°, and 30°, and e–h are that of cone angles of 20°, 30°, 40°, and 50°, respectively. The enhancement between the tip and substrate decreases with increased tilt and cone angles. The white lines indicate the interface of substrate.

possibilities to get a better result by employing a designed complex optical field to achieve a higher field intensity to improve the detection sensitivity.

For another, resolution is also an important evaluation index for TERS researches. As the excited hotspot is highly localized on the tip, it provides a high spatial resolution (full width at half-maximum of the hotspot) much smaller than the size of the tip apex [36]. The resolution is always closely related to the tip geometry and substrate material, and can be improved dramatically by sharping the tip and employing metallic substrate. For the optimized Au coating thickness here, in fact, the resolution still has space for improvement. Nevertheless, it can be competent for the most qualitative detections, these results could also provide a guiding significance for further TERS researches.

## 4. Conclusion

In summary, we established an inverted AFM-based TERS setup with illumination from the bottom to investigate the enhancement effect of Au claddings on Raman scattering spectroscopy. A gold coating with different thicknesses is cladded on the silicic AFM probe by thermal evaporation method with a slow deposition velocity followed with an annealing process. The probe is located at the longitudinal maxima point of the focused laser field to excite hotspot exactly in the gap between the tip and substrate. Both numerical simulations and experiments demonstrated that the cladding thickness has high effect on Raman spectrum enhancement, and an optimized thickness of 50 nm was achieved for the probe under experimental conditions. Furthermore, other factors are further analyzed to get a better enhancement, which will be implemented in the following works. This work gives out a practical guide to optimize the probes to improve the TERS sensitivity and could exert potentials in further TERS applications.

## Acknowledgements

This work was supported by the National Natural Science Foundation of China (61427819, 91750205, 61605117, 61805154, and 11604182) and the National Key Basic Research Program of China (973) (2015CB352004); X. Yuan appreciates the support given by the leading talents of Guangdong province program No. 00201505; X. Yuan, C. Min, and Y. Zhang acknowledge the Natural Science Foundation of Guangdong Province (2016A030312010, 2016A030310063, 2017A030313351), the Science and Technology Innovation Commission of Shenzhen (KQTD2017033011044403, ZDSYS201703031605029, JCYJ2017818144338999). We thank Dr. Yifeng Shao of Delft university of technology for his useful discussion.

## References

[1] R.M. Stöckle, Y.D. Suh, V. Deckert, R. Zenobi, Nanoscale chemical analysis by tip-enhanced Raman spectroscopy, Chem. Phys. Lett. 318 (2000) 131–136.
[2] J. Steidtner, B. Pettinger, Tip-enhanced Raman spectroscopy and microscopy on single dye molecules with 15 nm resolution, Phys. Rev. Lett. 100 (2008) 236101.
[3] E. Bailo, V. Deckert, Tip-enhanced Raman scattering, Chem. Soc. Rev. 37 (2008) 921–930.
[4] W. Zhang, B.S. Yeo, T. Schmid, R. Zenobi, Single molecule tip-enhanced Raman spectroscopy with silver tips, J. Phys. Chem. C 111 (2007) 1733–1738.
[5] Lingyan Meng, Mengtao Sun, Tip-enhanced photoluminescence spectroscopy of monolayer MoS2, Photon. Res. 5 (2017) 745–749.
[6] R. Treffer, R. Böhme, T. Deckert-Gaudig, K. Lau, T. Stephan, X. Lin, V. Deckert, Advances in TERS (tip-enhanced Raman scattering) for biochemical applications, Biochem. Soc. Trans. 40 (2012) 609–614.
[7] R. Zhang, Y. Zhang, Z.C. Dong, S. Jiang, C. Zhang, L.G. Chen, L. Zhang, Y. Liao, J. Aizpurua, Y. Luo, J.L. Yang, J.G. Hou, Chemical mapping of a single molecule by plasmon-enhanced Raman scattering, Nature 498 (2013) 82.
[8] Y. Saito, P. Verma, K. Masui, Y. Inouye, S. Kawata, Nano-scale analysis of graphene layers by tip-enhanced near-field Raman spectroscopy, J. Raman Spectrosc. 40 (2009) 1434–1440.
[9] T. Schmid, L. Opilik, C. Blum, R. Zenobi, Nanoscale chemical imaging using tip-enhanced Raman spectroscopy: a critical review, Angew. Chem. Int. Ed. 52 (2013) 5940–5954.
[10] T. Yano, P. Verma, Y. Saito, T. Ichimura, S. Kawata, Pressure-assisted tip-enhanced Raman imaging at a resolution of a few nanometres, Nat. Photonics 3 (2009) 473.
[11] J.H. Zhong, X. Jin, L. Meng, X. Wang, H.S. Su, Z.L. Yang, C.T. Willams, B. Ren, Probing the electronic and catalytic properties of a bimetallic surface with 3 nm resolution, Nat. Nanotechnol 12 (2017) 132–136.
[12] A.L. Demming, F. Festy, D. Richards, Plasmon resonances on metal tips: understanding tip-enhanced Raman scattering, J. Chem. Phys. 122 (2005) 184716.
[13] N. Hayazawa, Y. Saito, S. Kawata, Detection and characterization of longitudinal field for tip-enhanced Raman spectroscopy, Appl. Phys. Lett. 85 (2004) 6239–6241.
[14] W. Zhang, B. Yeo, T. Schmid, C. Hafner, R. Zenobi, Nanoscale roughness on metal surfaces can increase tip-enhanced Raman scattering by an order of magnitude, Nano Lett. 7 (2007) 1401–1405.
[15] Hailong Wang, Yuyang Wang, Yi Wang, Weiqing Xu, Shuping Xu, Modulation of hot regions in waveguide-based evanescent-field-coupled localized surface plasmons for plasmon-enhanced spectroscopy, Photon. Res 5 (2017) 527–535.
[16] A. Downes, D. Salter, A. Elfick, Finite element simulations of tip-enhanced Raman and fluorescence spectroscopy, J. Phys. Chem. B 110 (2006) 6692–6698.
[17] B. Pettinger, K.F. Domke, D. Zhang, G. Picardi, R. Schuster, Tip-enhanced Raman scattering: influence of the tip-surface geometry on optical resonance and enhancement, Surf. Sci. 603 (2009) 1335–1341.
[18] M.S. Anderson, Locally enhanced Raman spectroscopy with an atomic force microscope, Appl. Phys. Lett. 76 (2000) 3130–3132.
[19] M. Micic, N. Klymyshyn, Y.D. Suh, H.P. Lu, Finite element method simulation of the field distribution for AFM tip-enhanced surface-enhanced Raman scanning microscopy, J. Phys. Chem. B 107 (2003) 1574–1584.
[20] M. Asghari-Khiavi, B.R. Wood, P. Hojati-Talemi, A. Downes, D. McNaughton, A. Mechler. Exploring the origin of tip-enhanced Raman scattering; preparation of efficient TERS probes with high yield, J. Raman Spectrosc. 43 (2012) 173–180.
[21] Z. Zeng, S. Huang, D. Wu, L. Meng, M. Li, T. Huang, J. Zhong, X. Wang, Z. Yang, B. Ren, Electrochemical tip-enhanced Raman spectroscopy, J. Am. Chem. Soc. 137 (2015) 11928–11931.
[22] L. Meng, T. Huang, X. Wang, S. Chen, Z. Yang, B. Ren, Gold-coated AFM tips for tip-enhanced Raman spectroscopy: theoretical calculation and experimental demonstration, Opt. Express 23 (2015) 13804–13813.
[23] B. Ren, G. Picardi, B. Pettinger, Preparation of gold tips suitable for tip-enhanced Raman spectroscopy and light emission by electrochemical etching, Rev. Sci. Instrum. 75 (2004) 837–841.
[24] C.L. Cheung, J.H. Hafner, C.M. Lieber, Carbon nanotube atomic force microscopy tips: direct growth by chemical vapor deposition and application to high-

resolution imaging, Proc. Natl. Acad. Sci. 97 (2000) 3809–3813.
[25] C. Ropers, C.C. Neacsu, T. Elsaesser, M. Albrecht, M.B. Raschke, C. Lienau, Grating-coupling of surface plasmons onto metallic tips: a nanoconfined light source, Nano Lett. 7 (2007) 2784–2788.
[26] K. Tomita, Y. Kojima, F. Kannari, Selective coherent anti-Stokes Raman scattering microscopy employing dual-wavelength nanofocused ultrafast plasmon pulses, Nano Lett. 18 (2018) 1366–1372.
[27] T.R. Albrecht, S. Akamine, T.E. Carver, C.F. Quate, Microfabrication of cantilever styli for the atomic force microscope, J. Vac. Sci. Technol. A Vac. Surf. Films 8 (1990) 3386–3396.
[28] Y. Hirata, S. Yabuki, F. Mizutani, Application of integrated SECM ultra-micro-electrode and AFM force probe to biosensor surfaces, Bioelectrochemistry 63 (2004) 217–224.
[29] L.K. Yang, T.X. Huang, Z.C. Zeng, M.H. Li, X. Wang, F.Z. Yang, B. Ren, Rational fabrication of a gold-coated AFM TERS tip by pulsed electrodeposition, Nanoscale 7 (2015) 18225–18231.
[30] T.X. Huang, S.C. Huang, M.H. Li, Z.C. Zeng, X. Wang, B. Ren, Tip-enhanced Raman spectroscopy: tip-related issues, Anal. Bioanal. Chem. 407 (2015) 8177–8195.
[31] T.X. Huang, C.W. Li, L.K. Yang, J.F. Zhu, X. Yao, C. Liu, K.Q. Lin, Z.C. Zeng, S.S. Wu, X. Wang, F.Z. Yang, B. Ren, Rational fabrication of silver-coated AFM TERS tips with a high enhancement and long lifetime, Nanoscale 10 (2018) 4398–4405.
[32] B. Richards, E. Wolf, Electromagnetic diffraction in optical systems, II. Structure of the image field in an aplanatic system, Proc. R. Soc. Lond. A 253 (1959) 358–379.
[33] N. Kazemi-Zanjani, S. Vedraine, F. Lagugné-Labarthet, Localized enhancement of electric field in tip-enhanced Raman spectroscopy using radially and linearly polarized light, Opt. Express 21 (2013) 25271–25276.
[34] R. Ossikovski, Q. Nguyen, G. Picardi, Simple model for the polarization effects in tip-enhanced Raman spectroscopy, Phys. Rev. B 75 (2007) 045412.
[35] P. Verma, Tip-enhanced Raman spectroscopy: technique and recent advances, Chem. Rev. 117 (2017) 6447–6466.
[36] Z. Yang, J. Aizpurua, H. Xu, Electromagnetic field enhancement in TERS configurations, J. Raman Spectrosc. 40 (2009) 1343–1348.